ORIGINAL ARTICLE

CrossMark

Chlorella vulgaris integrates photoperiod and chloroplast redox signals in response to growth at high light

Lauren Hollis[1] · Alexander G. Ivanov[1,2] · Norman P. A. Hüner[1]

Abstract

Main conclusion **Photoacclimation to variable light and photoperiod regimes in *C. vulgaris* represents a complex interplay between "biogenic" phytochrome-mediated sensing and "operational" redox sensing signaling pathways.**

Chlorella vulgaris Beijerinck UTEX 265 exhibits a yellow–green phenotype when grown under high light (HL) in contrast to a dark green phenotype when grown at low light (LL). The redox state of the photosynthetic electron transport chain (PETC) as estimated by excitation pressure has been proposed to govern this phenotypic response. We hypothesized that if the redox state of the PETC was the sole regulator of the HL phenotype, *C. vulgaris* should photoacclimate in response to the steady-state excitation pressure during the light period regardless of the length of the photoperiod. As expected, LL-grown cells exhibited a dark green phenotype, low excitation pressure ($1-qP=0.22\pm0.02$), high chlorophyll (Chl) content (375 ± 77 fg Chl/cell), low Chl *a/b* ratio (2.97 ± 0.18) as well as high photosynthetic efficiency and photosynthetic capacity regardless of the photoperiod. In contrast, *C. vulgaris* grown under continuous HL developed a yellow–green phenotype characterized by high excitation pressure ($1-qP=0.68\pm0.01$), a relatively low Chl content (180 ± 53 fg Chl/cell), high Chl *a/b* ratio (6.36 ± 0.54) with concomitantly reduced light-harvesting polypeptide abundance, as well as low photosynthetic capacity and efficiency measured on a per cell basis. Although cells grown under HL and an 18 h photoperiod developed a typical yellow–green phenotype, cells grown at HL but a 12 h photoperiod exhibited a dark green phenotype comparable to LL-grown cells despite exhibiting growth under high excitation pressure ($1-qP=0.80\pm0.04$). The apparent uncoupling of excitation pressure and phenotype in HL-grown cells and a 12 h photoperiod indicates that chloroplast redox status cannot be the sole regulator of photoacclimation in *C. vulgaris*. We conclude that photoacclimation in *C. vulgaris* to HL is dependent upon growth history and reflects a complex interaction of endogenous systems that sense changes in photoperiod as well as photosynthetic redox balance.

Keywords Photosynthetic electron transport · Excitation pressure · Green algae · Photoperiod · Photoacclimation · Photosynthetic redox balance

✉ Norman P. A. Hüner
nhuner@uwo.ca

1 Department of Biology and The Biotron Centre for Experimental Climate Change Research, University of Western Ontario, London N6A 5B7, Canada

2 Institute of Biophysics and Biomedical Engineering, Bulgarian Academy of Sciences, 1113 Sofia, Bulgaria

Introduction

Differences in light quality are sensed by photosynthetic organisms through specialized blue light sensitive cryptochromes, phototropins and zeitlupe, and red light sensitive phytochromes (Möglich et al. 2010; Casal 2013; Kianian-momeni and Hallmann 2014). These photoreceptors serve a vital role in photoautotrophic growth and development by regulating the biosynthesis and assembly of thylakoid membranes and associated protein complexes during chloroplast biogenesis as well as photomorphogenesis; the photoreceptor-mediated sensing and signalling pathways that enable responses to light quality are defined as "biogenic" controls

(Pogson et al. 2008; Pogson and Albrecht 2011; Estavillo et al. 2012). In addition to photoreceptor-mediated light quality sensing, photoautotrophs also sense changes in their light environment through changes in photon flux density (PFD) (Sukenik et al. 1988; Laroche et al. 1991; Anderson et al. 1995; Durnford and Falkowski 1997; Pfannschmidt et al. 1999; Falkowksi and Chen 2003; Chen et al. 2004; Demmig-Adams et al. 2012; Stewart et al. 2015; Dietz 2015; Borisova-Mubarakshina et al. 2015). Changes in light energy availability are sensed by mature chloroplasts through modulation of the reduction–oxidation (redox) state of intersystem photosynthetic electron transport (Allen et al. 1995; Escoubas et al. 1995; Anderson et al. 1995; Durnford and Falkowski 1997; Hüner et al. 1998; Pfannschmidt 2003; Hüner et al. 2003; Chen et al. 2004; Ensminger et al. 2006; Bode et al. 2016) as well as the trans-thylakoid ΔpH in a time-dependent manner (Falkowksi and Chen 2003; Chen et al. 2004). However, recent evidence indicates that the acceptor-side of PSI rather than the intersystem electron transport PQ pool is the major source of redox signals that appear to be transduced through a ROS signal transduction pathway (Piippo et al. 2006; Borisova-Mubarakshina et al. 2015; Bode et al. 2016).

Despite their role in light-quality sensing, it has been demonstrated that photoreceptors do not play a major role in photoacclimation of the photosynthetic apparatus in mature chloroplasts. Walters et al. (1999) used *Arabidopsis thaliana* phytochrome mutants to demonstrate that adjustments to the structure and functionality of the photosynthetic apparatus in response to changing irradiance occur independently of light quality sensing through photoreceptors. Fey et al. (2005) further demonstrated redox signals from the photosynthetic apparatus are capable of inducing changes in nuclear-encoded gene expression independently of signalling mediated by photoreceptors. Rather, signals derived from the mature chloroplast are believed to act as the major regulators of photoacclimation (Escoubas et al. 1995; Hüner et al. 1998; Walters et al. 1999; Pfannschmidt 2003; Falkowksi and Chen 2003; Chen et al. 2004; Fey et al. 2005, Dietz, 2015; Bode et al. 2016).

Optimal photoautotrophic performance requires a balance between the energy obtained through photochemistry with the energy required for metabolism, growth and development. Imbalances in cellular energy flow occur whenever the rate of light energy absorption and transformation by temperature-insensitive photochemistry exceeds the capacity to dissipate excess light energy as heat through the xanthophyll cycle and/or utilize absorbed light energy through carbon, nitrogen and sulfur metabolism, respiration and ultimately growth (Hüner et al. 1998; Pfannschmidt 2003; Fey et al. 2005; Ensminger et al. 2006; Hüner et al. 2012; Dietz 2015). Changes in cellular energy balance are sensed as changes in the redox state of photosynthetic electron transport and can

be quantified as modulation of photosystem II (PSII) excitation pressure (Hüner et al. 1998).

Exposure of photoautotrophs to excessive excitation energy (EEE) (Karpinski et al. 1999) modulates excitation pressure which is a measure of the redox state of quinone A (Q_A), the first stable electron acceptor of PSII, and is estimated in vivo by the room temperature chlorophyll (Chl) a fluorescence induction parameter as $1 - qP$ where qP estimates the proportion of reduced Q_A as $Q_{A(reduced)}/(Q_{A(reduced)} + Q_{A(oxidized)})$ (Dietz et al. 1985; Hüner et al. 1998). Since the oxidation of $Q_{A(reduced)}$ via the intersystem PQ pool is considered the rate-limiting step in photosynthetic electron transport (Haehnel 1984; Ke 2001), the excitation pressure reflects the redox state of the intersystem photosynthetic electron transport chain (PETC) (Hüner et al. 2012; Bode et al. 2016). Sensing and signalling upon exposure to EEE by mature chloroplasts is defined as "operational" control (Pogson et al. 2008; Pogson and Albrecht 2011; Estavillo et al. 2012). These signals coordinate regulation of the structure and efficiency of the photosynthetic apparatus in mature, fully developed cells to ensure optimal photosynthetic performance while mitigating the harmful effects of excess light energy in the face of an ever-changing environment (Sukenik et al. 1987, 1988; Melis 1991; Tanaka and Melis 1997; Anderson et al. 1995; Falkowksi and Chen 2003; Matsuda et al. 2003; Pogson et al. 2008; Dietz 2015). In this manner, the mature chloroplast serves dual roles; both as an energy transducer and as a sensor for changes in the environment (Anderson et al. 1995; Hüner et al. 1998, Murchie et al. 2009; Brautigam et al. 2009; Hüner et al. 2012; Dietz 2015; Dietz et al. 2016; Hüner et al. 2016).

Research in the green algae *Dunaliella* sp. (Escoubas et al. 1995; Maxwell et al. 1995b; Król et al. 1997) and *Chlorella vulgaris* (Maxwell et al. 1994, 1995a; Wilson and Hüner 2000) indicate that the central sensor for changes in cellular energy poise of photosynthetic electron transport in green algae is the redox state of the plastoquinone (PQ) pool. This was based on the observation that a typical high light (HL) phenotype, characterized by yellow–green pigmentation, relatively low Chl content per cell and relatively high Chl *a/b* ratio with concomitantly reduced abundance of the major pigment-binding light-harvesting complex polypeptides associated with PSII (LHCII) could be mimicked by application of the herbicide 2,5-dibromo-3-methyl-6-isopropyl-1,4-benzoquinone (DBMIB) in the green algae *D. tertiolecta* (Escoubas et al. 1995; Chen et al. 2004) and *C. vulgaris* (Wilson et al. 2003). DBMIB mimics the effects of HL on the redox state of the PQ pool by inhibiting its oxidation by the Cyt b_6/f complex and subsequent transfer of electrons to PSI thereby keeping the PQ pool reduced in the light and results in a HL phenotype. In contrast, cultures developed a dark green, LL phenotype characterized by a relatively low Chl *a/b* ratio and high cellular Chl content per cell

when treated with 3-(3,4-dichlorophenyl)-1,1-dimethylurea (DCMU) whereby PSI keeps the PQ pool oxidized in the light because DCMU blocks the transfer of electrons from Q_A to quinone B (Q_B) and subsequently to the intersystem PQ pool (Sukenik et al. 1987, 1988; Anderson et al. 1995; Escoubas et al. 1995; Wilson et al. 2003; Chen et al. 2004; Kurepin et al. 2013; Petrillo et al. 2014). However, recent reports for *Arabidopsis thaliana* (Piippo et al. 2006; Athanasiou et al. 2010; Bode et al. 2016) and *Chlamydomonas reinhardtii* (Im and Grossman 2001; Humby et al. 2009) indicate that the intersystem PQ pool is probably not the primary site for the generation of redox signals involved in retrograde regulation. Rather, the acceptor-side of PSI appears to a major site for the generation of chloroplast redox signals (Dietz 2015, 2016; Bode et al. 2016).

The yellow–green, HL phenotype in *Chlorella vulgaris* can additionally be mimicked by growth at low temperature (Maxwell et al. 1994, 1995a, b; Król et al. 1997; Wilson and Hüner 2000; Wilson et al. 2003). Since light energy absorption and subsequent utilization in metabolism, respiration and growth integrates extremely fast, temperature-independent photochemistry with much slower, temperature-dependent biochemistry, the reduction state of Q_A can be modulated in a similar fashion by either low temperature or HL. High light will increase the rate of Q_A reduction through the increased PFD. Although low temperature, in the biologically relevant range, affects photochemistry minimally, low temperature limits the reaction rates of the temperature-sensitive, enzyme-mediated metabolic reactions on the acceptor-side of PSI that consume photosynthetically generated electrons. Therefore, low temperature will cause an over-reduction of photosynthetic electron transport chain and an increase in PSII excitation pressure by limiting metabolism and growth.

Since the yellow–green phenotype can be mimicked by either HL or low temperature, photoacclimation in response to changes in EEE is sensed through the redox state of the PETC as opposed to light or temperature per se (Maxwell et al. 1994; Hüner et al. 1998; Dietz et al. 2016). Changes in cellular energy balance by either growth PFD or temperature will induce exposure to EEE which modulates the reduction state of the intersystem electron transport chain (PETC) and can be estimated as PSII excitation pressure. This will induce a photoacclimation response which reflects a retailoring of the structure and function of the photosynthetic apparatus (Sukenik et al. 1987, 1988; Melis 1991; Anderson et al. 1995; Escoubas et al. 1995; Tanaka and Melis 1997; Falkowksi and Chen 2003; Matsuda et al. 2003; Wilson et al. 2003; Chen et al. 2004; Kurepin et al. 2013; Petrillo et al. 2014; Dietz 2015). Furthermore, since nutrient limitations and water availability will also limit the capacity to consume photosynthetically generated electrons (Grossman et al. 1994; Wykoff et al. 1998) and increase excitation

pressure, all photosynthetic organisms acclimate to changes in their environment, in part, by sensing and responding to the redox state of the PETC, an important "operational" signal (Pogson et al. 2008; Dietz 2008; Brautigam et al. 2009; Dietz et al. 2016).

When photoautotrophs are in photostasis (Melis 1998), the rate of light-induced photochemistry is balanced by the capacity to consume photosynthetically generated electrons through metabolism and growth and/or dissipate excess absorbed light energy nonphotochemically as heat through the xanthophyll cycle and nonphotochemical quenching (NPQ) (Demmig-Adams and Adams 1992; Demmig-Adams et al. 2012, 2014; Horton et al. 1996; Horton and Ruban 2005; Robert et al. 2004; Murchie et al. 2009; Ruban et al. 2012). Under these conditions, PSII excitation pressure is low, the PQ pools remain oxidized as estimated by a relatively low $1 - qP$, and cultures of green algae display a typical dark green, low light (LL) phenotype in which PSII reaction centers essentially remain open (P680 Pheo Q_A). Environmental stresses including HL and low temperature cause an increase in excitation pressure by causing an imbalance between light energy absorption through photochemistry and the capacity for cellular energy use (Maxwell et al. 1994; Escoubas et al. 1995; Maxwell et al. 1995a; Wilson and Hüner 2000; Falkowksi and Chen 2003; Murchie et al. 2009). Under these conditions, the intersystem PETC becomes reduced and excitation pressure is high reflecting the accumulation of closed PSII reaction centres (P680$^+$ Pheo Q_A^-). *Dunaliella tertiolecta* cultures acclimated to HL (Escoubas et al. 1995; Chen et al. 2004) or *Chlorella vulgaris* acclimated to either low temperature or HL (Maxwell et al. 1994; Savitch et al. 1996) display a yellow–green pigmentation characterized by retrograde redox suppression of the nuclear-encoded *Lhcb* expression leading to decreased pigment-binding LHCII polypeptide abundance with concomitantly reduced cellular Chl content, increased Chl *a/b* ratio and high NPQ. The reduction in the accumulation of LHCII polypeptides combined with high NPQ protects the photosynthetic apparatus by decreasing the efficiency of light absorption and energy transfer to reaction centers. *C. vulgaris* and the cyanobacterium, *Plectonema boryanum*, photoacclimate to either HL or low temperature by adjusting the structure and function of the photosynthetic apparatus as they appear to be limited in their capacity to stimulate either growth rate (Miskiewicz et al. 2000; Wilson and Hüner 2000) or rates of carbon fixation (Savitch et al. 1996) in response to imbalances in cellular energy flow.

Photosynthetic organisms are subjected to short-term variations in the light environment due to changes in cloud and canopy cover, as well as long-term diurnal and seasonal changes in photoperiod. However, previous studies on acclimation to EEE in *C. vulgaris* have been conducted under constant illumination (Maxwell et al. 1994, 1995a; Wilson

and Hüner 2000; Wilson et al. 2003; Hollis and Hüner 2017). In addition to redox retrograde regulation (Escoubas et al. 1995; Maxwell et al. 1995b; Chory and Wu 2001; Chen et al. 2004; Koussevitzky et al. 2007; Dietz 2008; Dietz et al. 2016), the major nuclear-encoded light-harvesting complex genes have additionally been demonstrated to be regulated by other factors including the circadian clock (Millar et al. 1995; Rochaix 2014). In fact, recently a link between the circadian clock (McClung 2006) and the redox state of plants has been proposed (Guadagno et al. 2018). To determine the effects of changes in photoperiod on acclimation to EEE, cultures of *C. vulgaris* were grown at a constant temperature of 28 °C at either continuous LL (150 µmol photons m^{-2} s^{-1}) or continuous HL growth regime at 2000 µmol photons m^{-2} s^{-1} (Maxwell et al. 1994, 1995a) with decreasing photoperiods.

We predicted that during growth and development under alternating light:dark cycles, PSII excitation pressure should relax during the daily dark period as the absence of light will negate the accumulation of closed PSII reaction centres. We hypothesized that if the redox status of the PETC is the sole regulator of photoacclimation, and therefore, the HL phenotype, cultures of *C. vulgaris* should photoacclimate in response to the steady-state redox status of the PETC during the light period regardless of the length of the photoperiod. Contrary to our hypothesis, we show that photoacclimation in *C. vulgaris* is dependent upon both photoperiod and photosynthetic redox state. We report that the extension of a dark period from 0 to 12 h generates a dark-green LL phenotype in *C. vulgaris* even though excitation pressure did not relax but remained high. The apparent uncoupling between the chloroplast redox signal and the cell phenotype is discussed.

Materials and methods

Culture conditions

Cultures of *Chlorella vulgaris* Beijerinck (UTEX 265) were grown axenically in Bold's basal media (Nichols and Bold, 1965) modified according to Maxwell et al. (1994). Cultures were grown in 400 mL capacity Photobioreactor cultivation vessels (FMT 150) which were maintained at a constant temperature of 28 °C and light intensities of either 150 or 2000 µmol photons m^{-2} s^{-1} supplied by an equal combination of red and blue light emitting diodes as described previously (Hollis and Hüner 2017). Cultures were grown under continuous light (24 h photoperiod), an 18 h photoperiod or 12 h photoperiod in a 24 h cycle at both light intensities. The temperature and photoperiod regimes were maintained by the Photobioreactor control system (Photon System Instruments, Hogrova, Czech Republic) (Hollis and Hüner 2017).

Chlorophyll content

Total chlorophyll content and the chlorophyll *a/b* ratio were calculated as previously described (Maxwell et al. 1994). Pigments were extracted in 90% acetone (v/v) using a Mini-beadbeater (BioSpec, Bartleville, USA) and chlorophyll content was calculated according to the equations of Jeffrey and Humphrey (1975). To determine the chlorophyll content on a per cell basis, cells were counted using a PhytoCyt flow cytometer (C6) with C-Plus data acquisition software (Turner Designs, Sunnyvale, USA). For cultures grown under continuous light, measurements were taken during mid-log phase. For cultures grown under a photoperiod, measurements were taken immediately following the start of the light period during mid-log phase growth.

Measurements of oxygen evolution

Measurements of oxygen evolution and consumption were performed on 1.5 mL of stirred samples at 28 °C in the presence of 5 mM $NaHCO_3$. Measurements were performed using a DW2 oxygen electrode with a LH11/R light probe controlled by the OxyLab control unit and data were collected using the OxyLab 32 v.1.15 software (Hansatech Instruments, King's Lynn, UK) at a series of light intensities between 0 and 600 µmol photons m^{-2} s^{-1}. Photosynthetic rates were normalized on a per cell basis. For all photoperiods, measurements were taken within 2 h of the start of the light period in mid-log phase cells.

SDS-PAGE and immunoblotting

Samples were collected during mid-log phase immediately following the start of a light period, centrifuged at 5000×*g* for 5 min at 4 °C, frozen with liquid nitrogen and stored at − 80 °C. For cultures grown under continuous light, samples were collected during mid-log phase. For cultures grown under a photoperiod, samples were collected immediately following the end of a dark period during mid-log phase. Total protein was extracted with 90% (v/v/) acetone using a Mini-beadbeater (BioSpec, Bartlesville, USA) and pelleted by centrifugation at 16, 100×*g* for 5 min at 5 °C. The pellet containing the total polypeptide was solubilized with 4% (v/v) solubilization buffer [60 mM Tris–HCl (pH 6.8), 1% (v/v) glycerol and 4% (w/v) sodium dodecyl sulfate] at 37 °C to a 1:4 ratio of protein:sodium dodecyl sulfate. Protein concentration was determined using a Pierce BCA protein assay system (Thermo Scientific, Rockford, USA).

Prior to electrophoresis, samples containing 20 µg of protein were mixed with an equal volume of loading dye [2% (v/v) β-mercaptoethanol, 13% (v/v) glycerol and 0.5% (w/v) bromophenol blue, 1% (w/v) DTT], heated at 80 °C for 4 min before centrifugation at 16,100×*g* for 1 min to

remove any unsolubilized debris. Electrophoresis was performed using the discontinuous buffer system of Laemmli (1970) with a 5% (w/v) stacking gel and a 15% (w/v) resolving gel containing 6 M urea for 3 h at 75 V. The separated polypeptides were either stained with Coomassie blue [0.2% (w/v) Coomassie blue, 50% (v/v) methanol, 7% (v/v) acetic acid] at room temperature overnight or electrophoretically transferred to a nitrocellulose membrane (Bio-Rad, Hercules, USA) at 5 °C for 1 h at 100 V. The nitrocellulose membranes were then blocked in Block buffer [Tris buffered saline (20 mM Tris (pH 7.5), 150 mM NaCl), 5% (w/v) milk powder, 0.01% (v/v) Tween 20] overnight at 5 °C before being probed with one of the following polyclonal primary antibodies from Agrisera (Vännäs, Sweden): Lhca2 (1:2000 dilution), Lhcb2 (1:5000 dilution), PHYA (1:10,000), PIF3 (1:10,000 dilution), psaB (1:4000 dilution) and psbA (1:10,000 dilution); as well as Rubisco (1:5000 dilution), which was generated by NPAH. Following incubation with horseradish peroxidase-conjugated secondary antibodies (Sigma, St. Louis, USA; 1:2000 dilution) the antibody–protein complexes were visualized with the Amersham Biosciences enhanced chemiluminescence detection system (GE Healthcare, Little Chalfont, UK) and X-ray film (Fugi Film, Tokyo, Japan). The density of each band was quantified using ImageJ software v1.45 (http://rsbweb.nih.gov/ij/download.html) following the instructions provided by the manufacturer to determine relative changes in polypeptides abundance.

Room temperature chlorophyll a fluorescence induction

Chlorophyll a fluorescence induction measurements were performed on cells placed in a temperature controlled stirred cuvette using XE-PAM fluorometer (XE-PAM GDEB0146; Heinz Walz, Effeltrich, Germany) with an optical unit (ED-101US/M), a photodiode detector unit (XE-PD) and a PAM data acquisition system (PDA-100). Temperature was maintained at 28 °C through the use of a temperature control unit (US-T/R). Steady-state fluorescence parameters were determined by irradiating the sample with actinic light adjusted to the growth irradiance with a saturating pulse (2600 µmol photons m^{-2} s^{-1}, 800 ms) applied every 30 s for 5 min. For cultures grown under continuous light (CL) measurements were taken during mid-log phase. For cultures grown under a specific photoperiod, measurements were taken on mid-log phase cells immediately following the end of a dark period.

Excitation pressure was calculated as $1 - qP = (F_S - F_O')/(F_M' - F_O')$ and was used as an estimation of the redox state of the intersystem PETC (van Kooten and Snell 1990) where $1 - qP$ estimates the proportion of closed PSII reaction centres. Partitioning of absorbed light energy was calculated where photons absorbed by the PSII antenna allocated to

PSII photochemistry and photosynthetic electron transport was calculated as $\Phi_{PSII} = 1 - F_S/F_{M'}$, regulated ΔpH- and/or xanthophyll-dependent nonphotochemical quenching (NPQ) within the PSII antenna was calculated as $\Phi_{NPQ} = F_S/F_{M'} - F_S/F_M$ and the non-regulated, constitutive nonphotochemical energy dissipation (f, d) was calculated as $\Phi_{f,d} = F_S/F_M$ (Hendrickson et al. 2004).

Statistical analysis

A two-way analysis of variance (ANOVA) was conducted with irradiance and photoperiod as explanatory variables followed by a Tukey's honest significant difference (HSD) multiple compression post hoc test to determine overlapping means. If an insignificant interaction term between irradiance and photoperiod was determined, the main effects of each of the factors were examined. Data were visually inspected for normality and homogeneity of variance. If equality of variance was not determined, the data were log transformed to achieve equal variance; the log-transformed data were inspected for normality and equal variance. Chlorophyll a/b ratios were log transformed as log(chlorophyll a) − log(chlorophyll b) prior to statistical analysis. For statistical evaluation of energy partitioning, Φ_{NPQ} was omitted as all values for one group were close to zero and the values for energy partitioning were sum constrained. A value of 0.05 was considered significant throughout. All statistical analysis was conducted using the statistical software package R version 3.0.2.

Results

Effect of photoperiod on phenotype

During growth at 28/150 (°C/µmol photons m^{-2} s^{-1}), *C. vulgaris* developed a typical dark green LL phenotype regardless of photoperiod (Fig. 1a–c). Cells of *C. vulgaris* exhibited a typical yellow–green HL phenotype when grown at 28/2000 under continuous light (CL; 24L:0D) (Fig. 1d). Despite the introduction of a 6 h dark period, *C. vulgaris* grown at 28/2000 under an 18 h photoperiod (18L:6D) still exhibited a comparable yellow–green phenotype visually indistinguishable from cells grown at 28/2000 under CL (Fig. 1, compare d and e). However, the introduction of a 12 h dark period (12L:12D) caused *C. vulgaris* cells grown under HL to exhibit a dark green phenotype indistinguishable from LL-grown cells (Fig. 1; compare a, b and c–f).

Effect of photoperiod on excitation pressure

Figure 2 shows representative room temperature Chl a fluorescence induction traces for cells of *C. vulgaris* grown at

Fig. 1 Representative phenotype for cultures of *C. vulgaris* grown at 28 °C/150 μmol photons m^{-2} s^{-1} and 28 °C/2000 μmol photons m^{-2} s^{-1} under either 24 h, 18 h and 12 h photoperiods. Phenotype was assayed immediately following the end of a dark period during mid-log phase growth. **a** 28/150 24L:0D, **b** 28/150 18L:6D, **c** 28/150 12L:12D, **d** 28/2000 24L:0D, **e** 28/2000 18L:6D, **f** 28/2000 12L:12D where values represent temperature (°C)/irradiance (μmol photons m^{-2} s^{-1}) with length of light (L) and dark period (D) in a 24 h cycle
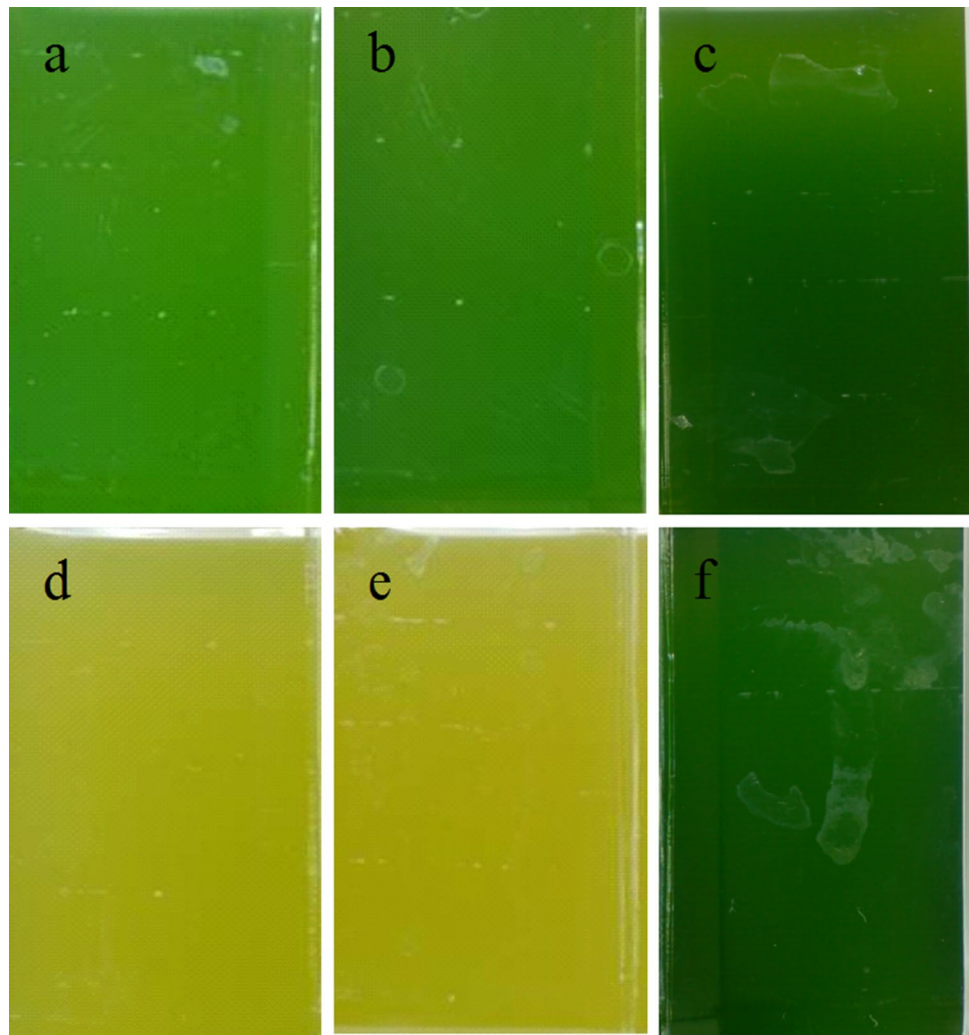
28/150 and 28/2000 under either CL, an 18 h photoperiod (18L:6D) or 12 h photoperiod (12L:12D). Excitation pressure was measured in vivo using the Chl *a* fluorescence parameter $1 - qP$ where $1 - qP$ estimates the proportion of closed PSII reaction centres (P680^{+} Pheo Q_{A}^{-}) (Dietz et al. 1985, Hüner et al. 1998). Cells of *C. vulgaris* grown at 28/15;0 exhibited comparable steady-state $1 - qP$ values of 0.22–0.27 during the light period which were approximately threefold lower than the steady-state of $1 - qP$ values of 0.69–0.82 exhibited by *C. vulgaris* grown at 28/2000 (irradiance, $p < 0.0001$, Tables 1, 2); however, within a growth light regime, there were no differences in $1 - qP$ across the various photoperiods. Therefore, when compared at the same photoperiod, *C. vulgaris* grown at 28/150 exhibited a relatively low PSII excitation pressure during the daily light period relative to cells grown at 28/2000. The length of the dark period had minimal effects on $1 - qP$ experienced during the day (Table 1).

At 28/150, typical fluorescence induction for *C. vulgaris* grown under 18 h and 12 h photoperiods closely resembled the fluorescence induction pattern characteristic of cells grown at 28/150 under CL (Fig. 2a–c). However, typical Chl *a* fluorescence induction traces for cells grown under CL at 28/2000 were characterized by an initial, but transient, quenching of the fluorescence signal below F_{o} upon illumination by the actinic light, followed by a slow rise of F_{S} during illumination with the actinic light to a steady-state level (F_{s}) accompanied by an almost complete quenching of $F_{M'}$ relative to cells grown under CL but 28/150 (Fig. 2, compare a–d). At 28/2000, fluorescence induction of cells grown under an 18 h photoperiod resembled the induction pattern characteristic of C. *vulgaris* grown at 28/2000 under CL (Fig. 2d, e). However, the introduction of a 12 h dark period at 28/2000 caused the initial, transient quenching of the fluorescence signal to disappear and the kinetics for the rise in F_{S} to more closely resemble the induction pattern characteristic of cells grown at 28/150 (Fig. 2, compare a,
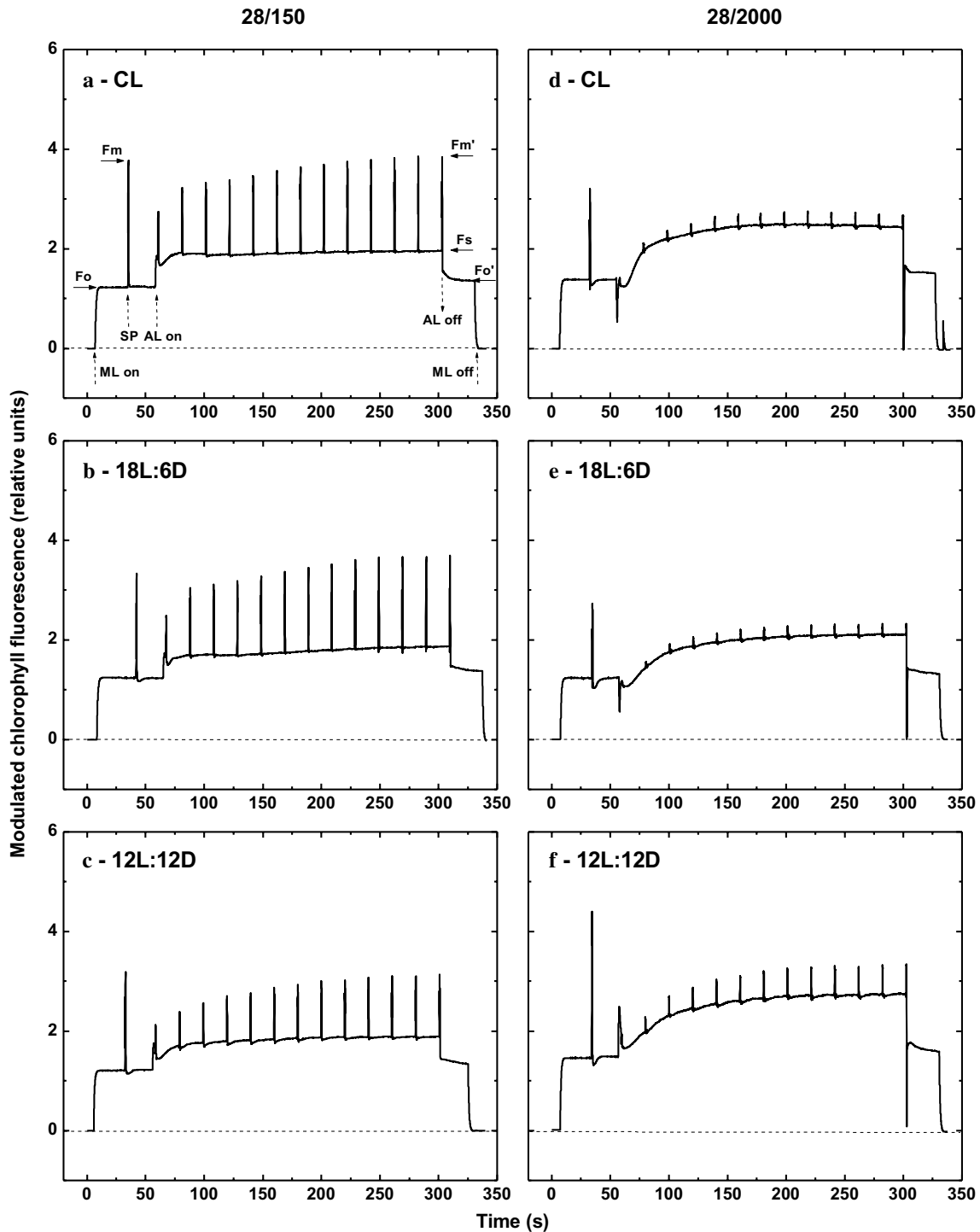
Fig. 2 Representative room temperature chlorophyll *a* fluorescence induction curves for *C. vulgaris* grown at 28 °C/150 µmol photons m^{-2} s^{-1} and 28 °C/2000 µmol photons m^{-2} s^{-1} with 24 h, 18 h and 12 h light periods in a 24 h cycle. **a** 28/150 24L:0D, **b** 28/150 18L:6D, **c** 28/150 12L:12D, **d** 28/2000 24L:0D, **e** 28/2000 18L:6D and **f** 28/2000 12L:12D where values indicate growth temperature (°C)/irradiance (µmol photons m^{-2} s^{-1}) and the length of light (L) and dark (D) periods in a 24 h cycle. *AL* actinic light, *ML* measuring light, *SP* saturating pulse

b and c–f); furthermore, the extent of the quenching of $F_{M'}$ appeared to be less severe than that of *C. vulgaris* at grown at 28/2000 under either CL or an 18 h photoperiod (Fig. 2e).

However, $F_{M'}$ for cells grown at 28/2000 and a 12 h photoperiod was still quenched relative to that observed for LL cells irrespective of photoperiod (Fig. 2).

Table 1 Chlorophyll characteristics and steady-state chlorophyll *a* fluorescence for cultures of *C. vulgaris* grown at 28 °C/150 µmol photons m^{-2} s^{-1} and 28 °C/2000 µmol photons m^{-2} s^{-1} with 24 h, 18 h and 12 h photoperiods

| | Growth regime | | | | | |
| | 28/150 | | | 28/2000 | | |
	24L:0D	18L:6D	12L:12D	24L:0D	18L:6D	12L:12D
F_V/F_M	0.67 ± 0.05^a	0.63 ± 0.03^a	0.64 ± 0.04^a	0.68 ± 0.06^a	0.59 ± 0.05^a	0.59 ± 0.07^a
Chl *a/b*	2.97 ± 0.18^b	3.11 ± 0.44^b	3.35 ± 0.16^b	6.36 ± 0.54^a	5.82 ± 0.53^a	3.17 ± 0.28^b
fg Chl/cell	375 ± 77^a	328 ± 67^a	338 ± 64^a	180 ± 53^b	126 ± 27^b	300 ± 15^a
1−qP	0.22 ± 0.02^b	0.25 ± 0.03^b	0.27 ± 0.03^b	0.69 ± 0.01^a	0.82 ± 0.02^a	0.80 ± 0.04^a

Numbers under growth regime indicate growth temperature (°C)/irradiance (µmol photons m^{-2} s^{-1}) and the length of the light (L) and dark (D) periods in a 24 h cycle. Values represent mean ± SEM; $n = 3$ expect Chl *a/b* where n = 5. Means were compared using a two-way ANOVA followed by a Tukey's HSD post hoc test; means not connected by the same letter are statistically different ($p < 0.05$)

$1 - qP$ photosystem II excitation pressure, *Chl* chlorophyll, F_V/F_M photosystem II photochemical efficiency

Table 2 Results for statistical analysis (two-way ANOVA) for *C. vulgaris* grown at 150 and 2000 µmol photons m^{-2} s^{-1} under either a 24 h, 18 h or 12 h photoperiod at 28 °C

Response variable	Source of variation	Result	Conclusion (Tukey's HSD post hoc test)
1−qP	I	$F_{1,12} = 99.9, p < 0.0001$	LL < HL
	PP	$F_{2,12} = 3.7, p = 0.0563$	
	I × PP	$F_{2,12} = 1.4, p = 0.283$	
Chl *a/b*	I	$F_{1,24} = 39.6, p < 0.0001$	
	PP	$F_{2,24} = 6.9, p = 0.00,413$	
	I × PP	$F_{2,24} = 13.3, p = 0.0001$	LL24 h = LL18 h = LL12 h = HL12 h < HL24 h = HL18 h
Chl cell^{-1}	I	$F_{1,12} = 36.1, p < 0.0001$	
	PP	$F_{2,12} = 5.0, p = 0.0263$	
	I × PP	$F_{2,12} = 4.6, p\ F_{2,12} = 4.6, p = 0.0324$	HL24 h = HL18 h < LL24 h = LL18 h = LL12 h = HL12 h
F_V/F_M	I	$F_{1,12} = 4.5, p = 0.0556$	
	PP	$F_{2,12} = 1.2, p\ F_{1,12} = 1.3, p = 0.325$	
	I × PP	$F_{2,12} = 0.2, p = 0.797$	
Φ_{PSII}	I	$F_{2,12} = 155.2, p < 0.0001$ HL < LL	
	PP	$F_{2,12} = 2.2, p = 0.160$	
	I × PP	$F_{2,12} = 0.717, p = 0.508$	
$\Phi_{f,d}$	I	$F_{2,12} = 7.4, p = 0.0188$	LL < HL
	PP	$F_{2,12} = 4.5, p = 0.0350$	24 h = 12 h < 18 h
	I × PP	$F_{2,12} = 1.7, p = 0.220$	
P_{MAX}	I	$F_{1,12} = 21.1, p = 0.0006$	
	PP	$F_{2,12} = 24.3, p < 0.0001$	
	I × PP	$F_{2,12} = 7.4, p = 0.008$	HL24 h = HL18 h < LL24 h = LL18 h = LL12 h = HL12 h
Slope	I	$F_{2,12} = 25.6, p = 0.0003$	
	PP	$F_{2,12} = 16.3, p = 0.0004$	
	I × PP	$F_{2,12} = 4.3, p = 0.0391$	HL24 h = HL18 h < LL24 h = LL18 h = LL12 h = HL12 h
Respiration	I	$F_{1,12} = 0.2, p = 0.694$	
	PP	$F_{2,12} = 2.0, p = 0.173$	
	I × PP	$F_{2,12} = 0.9, p = 0.439$	

$n = 3$; expect Chl *a/b* where $n = 5$

I, irradiance; PP, photoperiod; HL, high light, HL24 h, HL18 h and HL12 h; high light with 24 h, 18 h and 12 h photoperiod, respectively; LL, low light; LL24 h, LL18 h and LL12 h, low light with 24 h, 18 h and 12 h photoperiod, respectively

Effect of photoperiod of Chl content

Consistent with the dark green phenotype, cells of *C. vulgaris* grown at LL (28/150) exhibited comparably low Chl *a/b* ratios of 2.97–3.35 across all photoperiods (irradiance × photoperiod, $p = 0.0001$, Tukey's HSD $p > 0.05$, Tables 1, 2). Similarly, consistent with the yellow–green HL phenotype, cells grown at 28/2000 under either CL or an 18 h photoperiod exhibited twofold higher Chl *a/b* ratios of 6.36 and 5.82, respectively, relative to LL grown cells (Tukey's HSD $p < 0.05$, Tables 1, 2).

Compared to HL cells grown at 28/2000 under either CL or an 18 h photoperiod, *C. vulgaris* grown at HL but a 12 h photoperiod exhibited a twofold lower Chl *a/b* ratio (3.17) (Tukey's HSD $p < 0.05$, Table 2) despite growth and development at HL (Table 1); furthermore, the Chl *a/b* ratio exhibited by HL cells grown at 28/2000 under a 12 h photoperiod was similar to that of cells grown at LL (Tukey's HSD $p > 0.05$, Table 2).

A similar pattern for the effect of photoperiod was obtained for total cellular Chl content (irradiance × photoperiod, $p = 0.0234$, Tables 1, 2). Cells of *C. vulgaris* grown either at LL or HL with a 12 h photoperiod exhibited Chl contents that were approximately twofold higher (Tukey's HSD $p < 0.05$, Table 2) relative to HL cells grown at 28/2000 under either CL or an 18 h photoperiod (Table 1). These trends remained consistent irrespective of whether samples were taken at the start or end of the light period (Supp. Fig. S1). At 28/2000, when the photoperiod was increased above 12 h to either a 14 h or 16 h photoperiod the values obtained for the Chl *a/b* ratio, a proxy for phenotype, never yielded a clear pattern (Supp. Table S1); only when the photoperiod was increased to an 18 h light period did the phenotypic response become reproducible. Thus, the presence of the dark-green, LL phenotype, with concomitantly low Chl *a/b* ratio and high cellular Chl content, in *C. vulgaris* grown at HL but a 12 h photoperiod indicated an "uncoupling" of daytime PSII excitation pressure (Table 1) and the predicted phenotype.

Effect of photoperiod on polypeptide accumulation

The relative abundance of the representative light-harvesting complex polypeptide of PSII, Lhcb2, remained comparable across all photoperiods in *C. vulgaris* grown at LL at 28/150 (Fig. 3). The marked increase in the Chl *a/b* ratio in HL cells grown at 28/2000 under either CL or an 18 h photoperiod was reflected in an approximately 40% lower Lhcb2 polypeptide abundance relative to LL cells grown at all photoperiods (Fig. 3 and Table 1). In contrast, the low Chl *a/b* ratio in *C. vulgaris* grown at HL but a 12 h photoperiod was reflected in an approximately 30% increase in
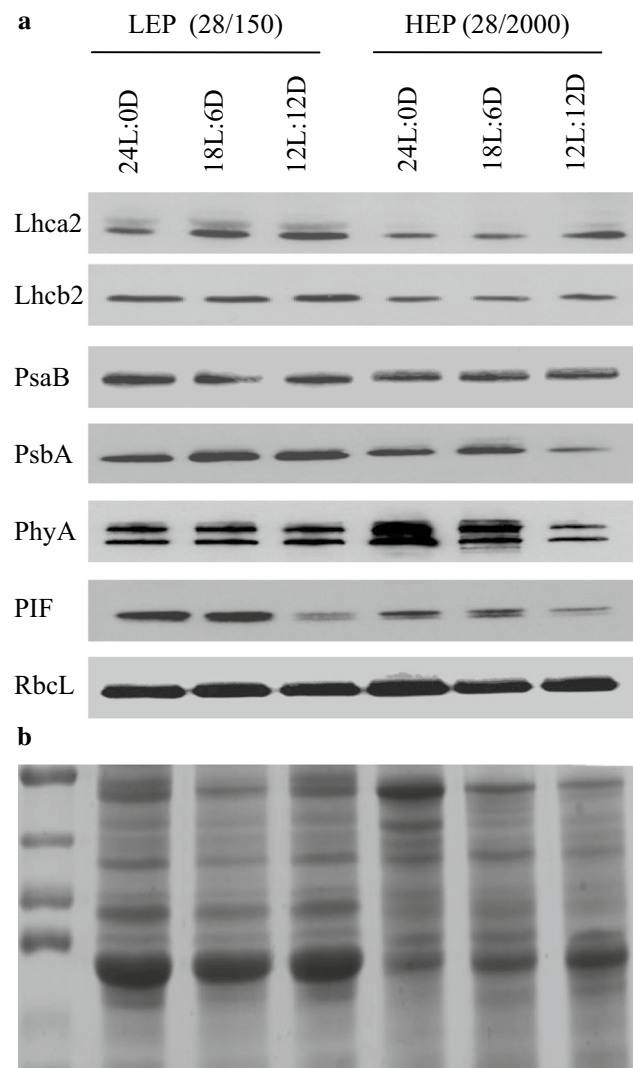

Fig. 3 Change in polypeptide abundance for cultures of *C. vulgaris* grown at low excitation pressure (LEP) at 28 °C/150 µmol photons m^{-2} s^{-1} and high excitation pressure (HEP) at 28 °C/2000 µmol photons m^{-2} s^{-1} with 24 h, 18 h and 12 h light periods in a 24 h cycle. Numbers above the immunoblots indicate growth temperature (°C)/irradiance (µmol photons m^{-2} s^{-1}) followed by the length of light (L) and dark (D) periods in a 24 h cycle. **a** Representative immunoblots against LHCI (Lhca2), LHCII (Lhcb2), PSI reaction centre polypeptide (PsaB), D1 polypeptide of PSII (PsbA), phytochrome A (PhyA), phytochrome interacting factor 3 (PIF3), and the large subunit of Rubisco (RbcL). **b** Representative Coomassie Brilliant Blue stained gel showing separated polypeptides; each lane was loaded with 20 µg of protein

Lhcb2 abundance relative to HL cells under either CL or an 18 h photoperiod (Fig. 3 and Table 1).

The abundance of the representative light harvesting polypeptide of PSI, Lhca2, followed a similar trend to that of Lhcb2 (Fig. 3). The abundance of Lhca2 was comparable across all photoperiods for LL cells, whereas HL cells grown under either CL or an 18 h photoperiod exhibited

approximately 43% and 61% decreases in Lhca2 abundance, respectively (Fig. 3). In contrast, Lhca2 abundance increased 2.5-fold during growth at 28/2000 but a 12 h photoperiod relative to cells grown at HL under either CL or an 18 h photoperiod (Fig. 3). Thus, *C. vulgaris* displayed a dark green phenotype at 28/150 which was mimicked by growth at HL but a 12 h photoperiod (Fig. 1). Concomitantly, these cells grown at HL but a 12 h photoperiod exhibited increases in Lhcb2 and Lhca2 polypeptide abundance relative to the yellow–green cells grown at HL under either CL or an 18 h photoperiod (Fig. 3).

While photoperiod did not affect the relative abundance of the representative PSII reaction centre polypeptide PsbA in cells grown at 28/150, PsbA levels were sensitive to photoperiod as a consequence of growth at HL and decreased by up to 45% with decreasing photoperiod at 28/2000; moreover, when compared at the same photoperiod, LL cells had a relatively greater abundance of PsbA polypeptides relative to HL cells (Fig. 3). However, minimal changes in the abundance of either PsaB, a representative PSI reaction centre polypeptide, or RbcL, the large-subunit of Rubisco, were detected regardless of growth PDF and photoperiod (Fig. 3). This indicated that not all plastid-localized polypeptides changed in abundance during growth and development under varying photoperiods in *C. vulgaris*.

Light quality perception mediated by light-sensitive photoreceptors such as phytochromes is critical for the generation of "biogenic" signals involved in photomorphogenesis (Pogson et al. 2008; Pogson and Albrecht 2011; Casal 2013; Kianianmomeni and Hallmann 2014). To assess the impact of the redox status of the PETC and photoperiod on components of phytochrome signalling the levels of phytochrome A (PHYA) and the phytochrome-interacting factor 3 (PIF3) were assessed (Fig. 3). There was a twofold decrease in the abundance of PIF3 in cells exposed to the 12 h photoperiod in both LL and HL cells as well as a threefold decrease in PHYA at the 12 h photoperiod in HL grown cells (Fig. 3).

Effect of photoperiod on PSII functionality

All cultures exhibited comparable maximum PSII photochemical efficiencies, as measured by F_V/F_M (Table 1) (irradiance, $p = 0.0556$; photoperiod $p = 0.325$, Table 2), indicating that none of the cultures were photoinhibited. Figure 4 demonstrates the response of excitation pressure, estimated as $1 - qP$, to increased measuring PFD. In all cultures, $1 - qP$ increased with increasing irradiance reflecting the closure of PSII reaction centres (Fig. 4). The maximum initial slope of the light response curves in Fig. 4 estimates of the number of photons required to convert an open PSII reaction centre (P680 Pheo Q_A) to a closed reaction centre (P680$^+$ Pheo Q_A^-), providing an estimate of the quantum requirement for PSII closure. The quantum requirement to close 50% of PSII
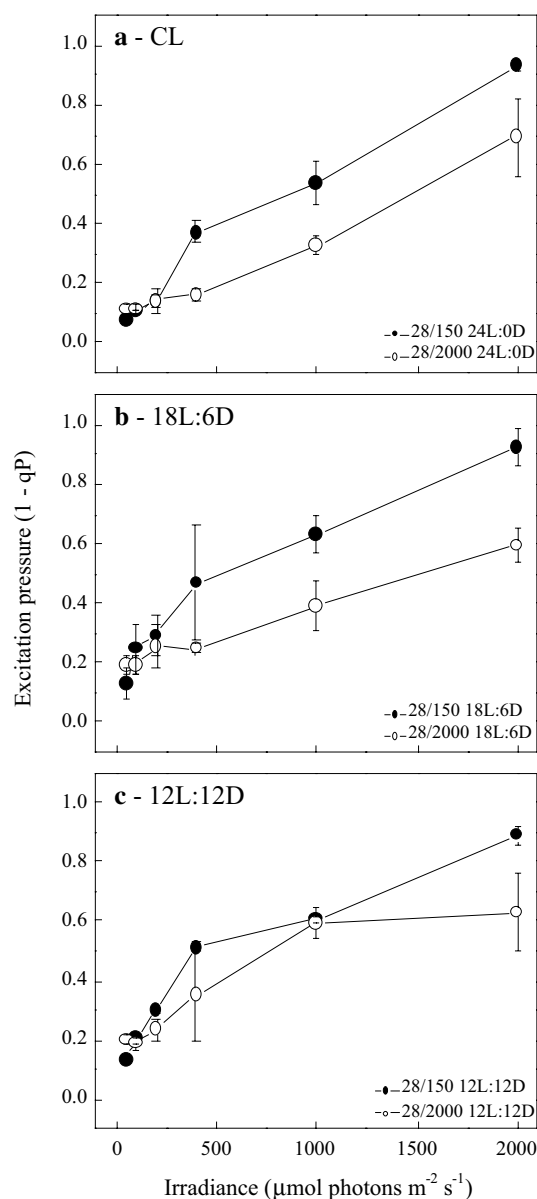

Fig. 4 Excitation pressure light responses curves for *C. vulgaris* grown at low excitation pressure (LEP; 28 °C/150 μmol photons m^{-2} s^{-1}) and high excitation pressure (HEP; 28 °C/2000 μmol photons m^{-2} s^{-1}) under: **a** continuous light (24L:0D), **b** 18 h photoperiod (18L:6D) or, **c** 12 h (12L:12D) photoperiod. Closed symbols represent LEP cells. Open symbols represent HEP cells. Numbers in the legends indicate temperature (°C)/irradiance (μmol photons m^{-2} s^{-1}) and the length of the light (L) and dark (D) periods in a 24 h cycle. Values represent mean ± SEM; $n = 3$

reaction centres in LL was about 574, 432 and 491 for the 24 h, 18 h and 12 h photoperiods, respectively (Fig. 4). The quantum requirement increased to approximately 700, 612 and 725 for HL *C. vulgaris* grown at either CL, a 18 h photoperiod or a 12 h photoperiod, respectively. The 22–48% increase in the quantum requirement for PSII closure for HL cells grown at 28/2000 relative to LL cells grown at 28/150
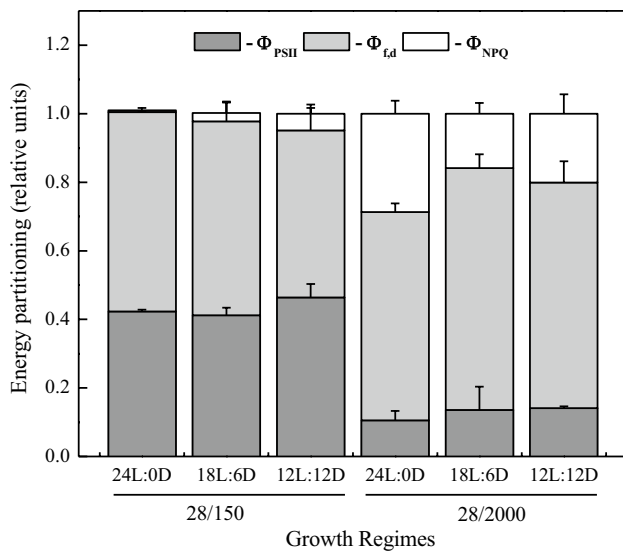
Fig. 5 Proportion of absorbed light energy consumed through photosystem II photochemistry (Φ_{PSII}) (dark gray), fluorescence and constitutive thermal dissipation ($\Phi_{f,d}$) (gray) and xanthophyll-dependent thermal dissipation (Φ_{NPQ}) (white) during steady-state photosynthesis for *C. vulgaris* grown at 28 °C/150 μmol photons m^{-2} s^{-1} and 28 °C/2000 μmol photons m^{-2} s^{-1} with 24 h, 18 h and 12 h light periods in a 24 h cycle. Numbers under bars indicate temperature (°C)/irradiance (μmol photons m^{-2} s^{-1}) and the length of the light (L) and dark (D) periods in a 24 h cycle. Values represent mean ± SEM; $n = 3$

Fig. 6 Oxygen evolution light response curves for *C. vulgaris* grown at low excitation pressure (LEP) at 28 °C/150 μmol photons m^{-2} s^{-1} and high excitation pressure (HEP) at 28 °C/2000 μmol photons m^{-2} s^{-1} under: **a** continuous light (CL; 24L:0D), **b** 18 h photoperiod (18L:6D) or, **c** 12 h photoperiod (12L:12D). Measurements presented are for gross oxygen evolution. Numbers in the legends indicate temperature (°C)/irradiance (μmol photons m^{-2} s^{-1}) and the length of the light (L) and dark (D) periods in a 24 h cycle. Values represent mean ± SEM; $n = 3$ (where not visible, error bars are smaller than the symbol)

but the same photoperiod reflects a decreased probability of reaction centre closure in cells grown at HL regardless of photoperiod.

HL cells of *C. vulgaris* grown at 28/2000 exhibited an approximately fourfold reduction in Φ_{PSII} (Fig. 5, black bars) (irradiance, $p < 0.0001$, Table 2) as well as an increase in the capacity to dissipate excess energy through regulated thermal dissipation through nonphotochemical quenching (Φ_{NPQ}) (Fig. 5, white bars). Furthermore, cells grown under HL exhibited a significantly higher capacity for energy dissipation through constitutive quenching (irradiance, $p = 0.0188$, Table 2) ($\Phi_{f,d}$) (Fig. 5, grey bars). When compared at the same photoperiod, *C. vulgaris* grown at HL under a 12 h photoperiod exhibited a 25% increase in the capacity for energy dissipation through constitutive quenching relative to cells grown at LL and the same photoperiod ($\Phi_{f,d}$) (Fig. 5). Therefore, while cells grown at HL under a 12 h photoperiod were similar to cells grown at LL in terms of pigmentation (Fig. 2), cellular Chl content (Table 1) and Lhcb2 levels (Fig. 3), they differed in the capacity for energy partitioning and more closely resembled cells grown at HL under either CL or an 18 h photoperiod (Fig. 5).
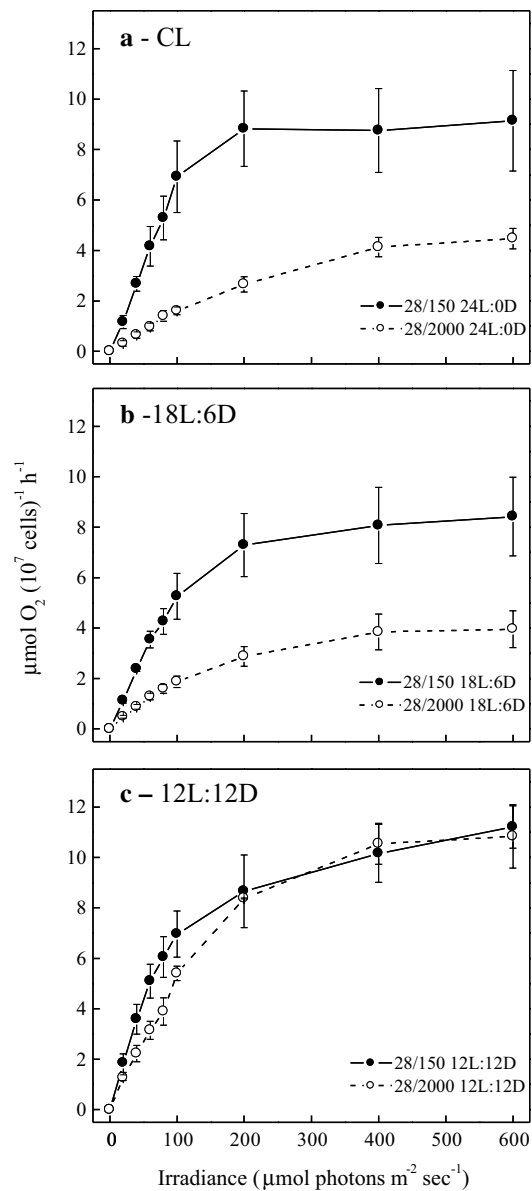
Effect of photoperiod on oxygen evolution

When grown under CL, the dark green LL cells of *C. vulgaris* grown at 28/150 (Fig. 6a, closed symbols) exhibited an approximately 2.5-fold higher maximum, light-saturated rate of oxygen evolution relative to the yellow–green

HL cells grown at CL but 28/2000 (Fig. 6a, open symbols) (irradiance × photoperiod, $p = 0.008$, Tukey's HSD $p = 0.010$, Table 2). Similar results were observed for cells grown at either LL or HL but an 18 h photoperiod (Tukey's HSD = 0.012, Table 2, Fig. 6b). However, under a 12 h photoperiod, *C. vulgaris* grown at 28/2000 exhibited comparable light-saturated rates of oxygen evolution relative to LL cells grown at 28/150 (Tukey's HSD $p = 0.99$, Table 2, Fig. 6c).

A similar trend for the effect of photoperiod on photosynthetic efficiency, calculated as the maximum initial slopes of the light response curves for oxygen evolution in Fig. 6a–c, was measured (irradiance × photoperiod, $p = 0.039$, Table 2). Photosynthetic efficiency was twofold higher in LL cells of *C. vulgaris* grown at 28/150 under either CL or an 18 h photoperiod relative to HL cells grown at 28/2000 under either CL (Tukey's HSD $p = 0.034$, Table 2) or an 18 h photoperiod, respectively (Tukey's HSD $p = 0.0026$), Table 2, Fig. 6a, b). Although photosynthetic efficiency tended to be higher in LL-grown than HL-grown cells under a 12 h photoperiod (Fig. 6c), this difference was not statistically different (Tukey's HSD $p = 0.425$, Table 2). However, neither growth PFD nor photoperiod significantly affected the rate of dark respiration (Table 3) (irradiance, $p = 0.694$; photoperiod, $p = 0.173$, Table 2).

Discussion

LHCII polypeptide abundance has been demonstrated to be reduced to a similar extent by either continuous HL (Sukenik et al. 1987, 1988; Melis 1991; Tanaka and Melis 1997; Falkowksi and Chen 2003; Matsuda et al. 2003; Chen et al. 2004), low temperature (Maxwell et al. 1994, 1995a, b; Escoubas et al. 1995; Król et al. 1997; Wilson et al. 2003) or DBMIB (Escoubas et al. 1995; Wilson et al. 2003; Bode et al. 2016) in plants and green algae. Based on these findings, it was concluded that LHCII accumulation is regulated by the redox state of the intersystem electron transport chain, measured by PSII excitation pressure, as opposed to light or temperature per se under steady illumination in green algae (Maxwell et al. 1994; Hüner et al. 1998; Wilson et al. 2003; Ensminger et al. 2006). These results are supported by the work of Walters and colleagues who demonstrated that photoacclimation of the photosynthetic apparatus of *A. thaliana* to changes in PFD occurs independently of sensing and signalling pathways mediated by photoreceptors in *A. thaliana* (Walters et al. 1999).

When cells were grown at LL, the duration of the daily photoperiod did not appear to influence the photoacclimation response in *C. vulgaris*. LL cells grown under either an 18 h photoperiod or 12 h photoperiod exhibited the dark green pigmentation (Fig. 1), high Chl per cell as well as low Chl *a/b* (Table 1) with concomitantly high LHCII abundance (Fig. 3) typical of cells acclimated under continuous LL and low excitation pressure. We suggest that despite the introduction of a dark period during growth and development at LL, PSII antenna size, as well as the associated phenotype appear to be insensitive to photoperiod.

In contrast, the length of the photoperiod had a distinct effect on the apparent PSII antenna size as measured by Chl and LHCII abundance as well as photosynthetic efficiency during growth at HL. Cells of *C. vulgaris* grown at HL under a 12 h photoperiod exhibited the dark-green phenotypic response (Fig. 1f) typical of growth and development under LL and displayed a characteristically high cellular Chl content per cell and low Chl *a/b* ratio (Table 1). However, since exposure of cells grown under CL at 28/2000 exhibited no consistent pattern when exposed to either a 14 h or 16 h photoperiod, we suggest that the lack of a consistent pattern in either Chl accumulation or Chl *a/b* ratios may indicate a photoperiod threshold to the photoacclimation response somewhere between the 18 h and 12 h photoperiod for cells grown under HL.

Table 3 Oxygen evolution for *C. vulgaris* grown at 28 °C/150 µmol photons m^{-2} s^{-1} and 28 °C/2000 µmol photons m^{-2} s^{-1} with 24 h, 18 h and 12 h photoperiods

	Growth regime					
	28/150			28/2000		
	24L:0D	18L:6D	12L:12D	24L:0D	18L:6D	12L:12D
P_{MAX}	9.80 ± 0.93[a]	8.95 ± 1.28[a]	9.19 ± 1.32[a]	4.06 ± 0.36[b]	3.17 ± 0.45[b]	9.80 ± 0.95[a]
Slope	0.04 ± 0.002[a]	0.05 ± 0.006[a]	0.05 ± 0.003[a]	0.02 ± 0.007[b]	0.02 ± 0.002[b]	0.05 ± 0.006[a]
Resp.	1.69 ± 0.42[a]	1.54 ± 0.39[a]	1.66 ± 0.50[a]	0.96 ± 0.24[a]	1.11 ± 0.32[a]	1.88 ± 0.19[a]

Numbers under growth regime indicate growth temperature (°C)/irradiance (µmol photons m^{-2} s^{-1}) and the length of the light (L) and dark (D) periods in a 24 h cycle. Values represent mean ± SEM; $n = 3$. Means were compared using a two-way ANOVA followed by Tukey's HSD test; means not connected by the same letter are statistically different ($p < 0.05$)

P_{MAX}, photosynthetic capacity [µmol O$_2$ evolved (10^7 cells]$^{-1}$ h^{-1})]; Resp., dark respiration [µmol O$_2$ consumed (10^7 cells)$^{-1}$ h^{-1}]; Slope, initial slope or photosynthetic efficiency [µmol O$_2$ (10^7 cells)$^{-1}$ (µmol photons m^{-2} s^{-1})$^{-1}$]

Despite the introduction of a 6 h dark period, HL cells of *C. vulgaris* grown at 28/2000 exhibited the yellow–green pigmentation (Fig. 1e), low Chl per cell and high Chl *a/b* (Table 1) with concomitantly reduced LHCII abundance (Fig. 3) as well as reduced photosynthetic capacity and efficiency (Fig. 6b) typical of cells acclimated to continuous HL. This indicates that cells of *C. vulgaris* grown at 28/2000 under an 18 h photoperiod both structurally and functionally mimic *C. vulgaris* photoacclimated to continuous HL. Although the introduction of a dark period should relax excitation pressure due to the absence of light energy required to close PSII reaction centres, these cells appear to remain locked in a HL-acclimated state despite the 6 h of darkness. Similarly, Post et al. (1984) demonstrated that photoacclimation in the cells of the diatom *Thalassiosira weisflogii* did not respond to the daily 12 h photoperiod as the cells did not photoacclimate in response to darkness; rather photoacclimation was correlated with the average PFD during the light period. These results are consistent with our recent report which showed that the relaxation of excitation pressure in *C. vulgaris* is light-dependent with an optimal PFD of 110 μmol photons $m^{-2}\,s^{-1}$ (Hollis and Hüner 2017).

Based on phenotype (Fig. 1), Chl content (Table 1), LHCII abundance (Fig. 3), as well as light response curves for O_2 evolution (Fig. 6), we conclude that *C. vulgaris* grown at HL and a 12 h photoperiod are both structurally and functionally comparable to cells grown at LL. However, with respect to energy partitioning (Fig. 5), cells grown under HL with a 12 h photoperiod were similar to HL cells. Surprisingly, HL cells grown under a 12 h photoperiod appeared to mimic, for the most part, the responses characteristic of photoacclimation to LL despite exposure to HL and high excitation pressure measured as 1 − qP. Thus, it appears that the regulation of phenotype in *C. vulgaris* UTEX 265 can be "uncoupled" from the relative redox state of the PETC by the duration of the photoperiod in HL-grown cells. Consequently, the redox state of the PETC cannot be the sole determinate of the HL phenotype and photoacclimation in *C. vulgaris* during growth and development under variable photoperiods. Contrary to previous reports that assume that excitation pressure alone governs photoacclimation in *C. vulgaris* (Maxwell et al. 1994, 1995a, b; Hüner et al. 1998; Wilson and Hüner 2000; Wilson et al. 2003; Hüner et al. 2012), we conclude that photoacclimation in *C. vulgaris* to HL must be both redox- and photoperiod-dependent.

Cells grown at 28/2000 are exposed to approximately 13-times more total photons during the 12 h light period relative to cells grown at 28/150 during a 12 h light period. Therefore, a mechanism must be in place to provide protection from the potential photodamage associated with prolonged exposure to high light. Normally, exposure to high light elicits short-term photoprotective mechanisms including the induction of the xanthophyll cycle that protect against photodamage of the photosynthetic apparatus by decreasing the efficiency of light energy transfer (Demmig-Adams and Adams III 2000; Demmig-Adams et al. 2012, 2014). Consistently, despite the phenotypic similarities to LL cells, *C. vulgaris* grown under HL and a 12 h photoperiod exhibit an 80% increase in $\varPhi_{NPQ}$ and a fourfold reduction in $\varPhi_{PSII}$ relative to cells grown at 28/150 irrespective of photoperiod (Fig. 5). Quenching of absorbed light energy through the xanthophyll cycle is considered to be the primary, inducible process contributing to photoprotection through nonphotochemical dissipation of excess light energy (Demmig-Adams and Adams 1992, 2000; Demmig-Adams et al. 2012, 2014; Stewart et al. 2015). Low lumenal pH results in the conversion of violaxanthin to zeaxanthin, the presence of which allows for thermal dissipation of excess excitation energy (Demmig-Adams et al. 2012; Gilmore and Yamamoto 1993). *C. vulgaris* grown at 28/2000 under a 12 h photoperiod also exhibits the greatest increase in the capacity for constitutive thermal dissipation ($\varPhi_{f,d}$) (Fig. 5). The mechanism for non-regulated constitutive quenching of excitation energy remains equivocal but it may reflect either the different proposed sites for antenna quenching (Jahns and Holzwarth 2012; Derks et al. 2015) or alternatively, may reflect PSII reaction centre quenching (Ivanov et al. 2003; Hüner et al. 2005; Sane et al. 2012). Therefore, *C. vulgaris* grown at HL and a 12 h photoperiod appears to represent an anomaly. Although the structure of the photosynthetic apparatus of *C. vulgaris* at grown 28/2000 under a 12 h photoperiod mimics LL cells grown at 28/150, in terms of the cellular capacity for energy dissipation, these cells are functionally comparable to HL-grown cultures.

The phenotypic and photosynthetic response of *C. vulgaris* grown at HL but a 12 h photoperiod relative to cells grown at LL was completely unexpected. Furthermore, the apparent sensitivity to a 12 h photoperiod in HL cells occurred despite the fact HL cells grown at a 12 h photoperiod were exposed to a daily photon exposure that was 13-fold greater than that of LL-grown cells regardless of photoperiod. This is consistent with the threefold higher excitation pressure exhibited by the HL cells compared to LL cells regardless of photoperiod (Table 1). Thus, differences in daily photon exposure cannot account for the photoperiodic sensitivity of HL cells of *C. vulgaris* since excitation pressure varied by only 16% (1 − qP = 0.69–0.80) for HL cells as a function of photoperiod. Thus, we suggest that photoperiod must contribute to the photoacclimation of HL cells of *C. vulgaris* independently of the redox state of the PETC. However, since photoacclimation of LL cells appeared to be insensitive to photoperiod, it appears that the photoperiod requirement in *C. vulgaris* is strictly dependent on the developmental history with respect to growth photon flux density.

During photomorphogenesis, photoreceptors provide light input signals to the circadian clock while phytochromes specifically enable responses the far-red/red range of light (McClung 2006; Casal 2013; Kianianmomeni and Hallmann 2014). Light-quality specific signal transduction is facilitated by phytochrome-specific target proteins including phytochrome-interacting factors (PIFs) (Shin et al. 2013). Interestingly, distinct responses for PHYA and the PIF3 in response to photoperiod were detected as both PIF3 and PHYA abundance decreased during growth under a 12 h photoperiod in cells grown at HL (Fig. 6). The reduced accumulation of both PhyA and PIF3 under a 12 h photoperiod may indicate a differential impact on the core oscillator and clock function in a manner that potentially influences clock output signals for photoacclimation under a 12 h photoperiod in HL-grown cells of *C. vulgaris*.

Length of the daily light period induces a distinct photosynthetic acclimation response in *C. vulgaris* grown at HL. This is analogous to research in *A. thaliana* where acclimation to a short-day photoperiod mimicked the structural responses, including increased Chl content, increased leaf biomass and decreased Chl *a/b* ratio, characteristic of shade acclimated leaves (Lepisto et al. 2009). Photoperiod has additionally been demonstrated to differentially influence the stress response to hydrogen peroxide and ozone in *A. thaliana* (Queval et al. 2007, 2012) and *Trifolium subterraneum* (Vollsnes et al. 2009), respectively. In *A. thaliana*, day length specific responses appear to be under the control of a genetic program as opposed to representing a response to differential exposure time to stressful conditions per se (Chaouch and Noctor 2010; Chaouch et al. 2010). Based on the distinct and discrete responses elicited by 18 h and 12 h photoperiods at HL, and the differential accumulation of PHYA and PIF3, we suggest that the phenotypic response to HL under either an 18 h or 12 h photoperiod in *C. vulgaris* likely involves an intrinsic photoperiodic response in addition to a photosynthetic redox response. It appears that photoperiod may play a crucial role in conditioning the acclimation response to a variety of environmental stresses in terrestrial plants such as *Arabidopsis thaliana* as well as *C. vulgaris*. Thus, acclimation to high light stress in *C. vulgaris* appears to be much more complex than previously assumed (Hüner et al. 1998, 2003; Ensminger et al. 2006; Hüner et al. 2012, 2013).

A consensus has emerged that "operational" signals derived from mature chloroplasts act as major regulators of phenotype through retailoring of the structure and composition of the photosynthetic apparatus (Sukenik et al. 1987, 1988; Laroche et al. 1991; Melis 1991; Anderson et al. 1995; Hüner et al. 1998; Pfannschmidt et al. 1999; Falkowksi and Chen 2003; Matsuda et al. 2003; Chen et al. 2004; Ensminger et al. 2006; Piippo et al. 2006; Hüner et al. 2012; Borisova-Mubarakshina et al. 2015; Dietz 2015; Stewart

et al. 2015; Bode et al. 2016). In this study, however, the apparent "uncoupling" of PSII excitation pressure and the expected photoacclimation response indicates that chloroplast redox status cannot be the sole regulator of photoacclimation under a variable light and photoperiod regime in *C. vulgaris*.

We conclude that photoacclimation to HL in *C. vulgaris* likely represents a complex interplay between "biogenic" phytochrome-mediated sensing and "operational" redox sensing signaling pathways (Pogson et al. 2008; Pogson and Albrecht 2011) consistent with the proposal of Guadagno et al. (2018). Signals pertaining to day length must be able to interact with, or override the photosynthetic redox signals to modify the photoacclimation response. Interaction between light-specific receptors and chloroplast redox signals during leaf acclimation in the terrestrial plant has been proposed (Ruckle et al. 2007; Ruckle and Larkin 2009; Guadagno et al. 2018). Similarly, the defective photoacclimation responses in the *det1* signal transduction mutant in *A. thaliana* does support some degree of cross-talk between photoreceptor-regulated responses and other regulators of photosynthetic acclimation (Walters et al. 1999). Currently, only fragments of these signalling pathways are known. The elucidation of cross-talk between photoreceptor-mediated "biogenic" pathways and plastid-mediated redox "operational" pathways and the extent to which cross-talk alters acclimation of the photosynthetic apparatus to different PFD and photoperiods remains to be elucidated.

References

Allen JF, Alexciev K, Hakansson G (1995) Regulation by redox signalling. Curr Biol 5:869–872. https://doi.org/10.1016/S0960-9822(95)00176-X

Anderson JM, Chow WS, Park YI (1995) The grand design of photosynthesis: acclimation of the photosynthetic apparatus to environmental cues. Photosynth Res 46:129–139

Athanasiou K, Dyson BC, Webster RE, Johnson GN (2010) Dynamic acclimation of photosynthesis increases plant fitness in changing environments. Plant Physiol 152:366–373. https://doi.org/10.1104/pp.109.149351

Bode R, Ivanov AG, Hüner NPA (2016) Global transcriptome analyses provide evidence that chloroplast redox state contributes to intracellular as well as long-distance signalling in response to stress and acclimation in Arabidopsis. Photosynth Res 128:287–312. https://doi.org/10.1007/s11120-016-0245-y

Borisova-Mubarakshina MM, Ivanov BN, Vetoshkina DV, Lubimov VY, Fedorchuk TP, Naydov IA, Kozuleva MA, Rudenko NN, Dall'Osto L, Cazzaniga S, Bassi R (2015) Long-term acclimatory response to excess excitation energy: evidence for a role of hydrogen peroxide in the regulation of photosystem II antenna size. J Exp Bot 66:7151–7164. https://doi.org/10.1093/jxb/erv410

Brautigam K, Dietzel L, Kleine T, Stroher E, Wormuth D, Dietz K-J, Radke D, Wirtz M, Hell R, Dormann P, Nunes-Nesi A, Schauer N, Fernie AR, Oliver SN, Geigenberger P, Leister D, Pfannschmidt T (2009) Dynamic plastid redox signals integrate gene expression and metabolism to induce distinct metabolic states in photosynthetic acclimation in Arabidopsis. Plant Cell 21:2715–2732. https://doi.org/10.1105/tpc.108.062018

Casal JJ (2013) Photoreceptor signaling networks in plant responses to shade. Annu Rev Plant Biol 64:403–427. https://doi.org/10.1146/annurev-arplant-050312-120221

Chaouch S, Noctor G (2010) Myo-inositol abolishes salicylic acid-dependent cell death and pathogen defence responses triggered by peroxisomal hydrogen peroxide. New Phytol 188:711–718. https://doi.org/10.1111/j.1469-8137.2010.03453.x

Chaouch S, Queval G, Vanderauwera S, Mhamdi A, Vandorpe M, Langlois-Meurinne M, Van Breusegem F, Saindrenan P, Noctor G (2010) Peroxisomal hydrogen peroxide is coupled to biotic defense responses by ISOCHORISMATE SYNTHASE1 in a daylength-related manner. Plant Physiol 153:1692–1705. https://doi.org/10.1104/pp.110.153957

Chen YB, Durnford DG, Koblizek M, Falkowski PG (2004) Plastid regulation of Lhcb1 transcription in the chlorophyte alga Dunaliella tertiolecta. Plant Physiol 136:3737–3750. https://doi.org/10.1104/pp.104.038919

Chory J, Wu D (2001) Weaving the complex web of signal transduction. Plant Physiol 125:77–80. https://doi.org/10.1104/pp.125.1.77

Demmig-Adams B, Adams WW III (1992) Photoprotection and other responses of plants to high light stress. Annu Rev Plant Physiol Plant Mol Biol 43:599–626. https://doi.org/10.1146/annurev.pp.43.060192.003123

Demmig-Adams B, Adams WW III (2000) Harvesting sunlight safely. Nature 403:373–374. https://doi.org/10.1038/35000315

Demmig-Adams B, Cohu CM, Muller O, Adams W III (2012) Modulation of photosynthetic energy conversion efficiency in nature: from seconds to seasons. Photosynth Res 113:75–88. https://doi.org/10.1007/s11120-012-9761-6

Demmig-Adams B, Stewart JJ, Burch TA, Adams WW III (2014) Insights from placing photosynthetic light harvesting into context. J Phys Chem Lett 5:2880–2889. https://doi.org/10.1021/jz5010768

Derks A, Schaven K, Bruce D (2015) Diverse mechanisms for photoprotection in photosynthesis. Dynamic regulation of photosystem II excitation in response to rapid environmental change. Biochem Biophys Acta 1847:468–485. https://doi.org/10.1016/j.bbabio.2015.02.008

Dietz KJ (2008) Redox signal integration: from stimulus to networks and genes. Physiol Plant 133:459–468

Dietz K (2015) Efficient high light acclimation involves rapid processes at multiple mechanistic levels. J Exp Bot 66:2901–2914. https://doi.org/10.1093/jxb/eru505

Dietz K, Schreiber U, Heber U (1985) The relationship between the redox state of Q_A and photosynthesis in leaves at various carbon-dioxide, oxygen and light regimes. Planta 166:219–226. https://doi.org/10.1007/BF00397352

Dietz K-J, Turkan I, Krieger-Liszkay A (2016) Redox- and reactive oxygen species-dependent signaling into and out of the photosynthesizing chloroplast. Plant Physiol 171:1541–1550

Durnford DG, Falkowski PG (1997) Chloroplast redox regulation of nuclear gene transcription during photoacclimation. Photosynth Res 53:229–241

Ensminger I, Busch F, Hüner NPA (2006) Photostasis and cold acclimation: sensing low temperature through photostasis. Physiol Plant 126:28–44. https://doi.org/10.1111/j.1399-3054.2006.00627.x

Escoubas JM, Lomas M, LaRoche J, Falkowski PG (1995) Light intensity regulation of cab gene transcription is signaled by the redox state of the plastoquinone pool. Proc Natl Acad Sci USA 92:10237–10241

Estavillo GM, Chan KX, Phua SY, Pogson BJ (2012) Reconsidering the nature and mode of action of metabolite retrograde signals from the chloroplast. Front Plant Sci 3:300. https://doi.org/10.3389/fpls.2012.00300

Falkowksi PG, Chen Y-B (2003) Photoacclimation of light harvesting systems in eukaryotic algae. In: Green BR, Green WW (eds) Advance in photosynthesis and respiration, light harvesting antennas in photosynthesis, vol 13. Kluwer Academic Publishers, Dordrecht, pp 423–447

Fey V, Wagner R, Brautigam K, Pfannschmidt T (2005) Photosynthetic redox control of nuclear gene expression. J Exp Bot 56:1491–1498. https://doi.org/10.1093/jxb/eri180

Gilmore AM, Yamamoto HY (1993) Linear models relating xanthophylls and lumen acidity to non-photochemical fluorescence quenching. Evidence that antheraxanthin explains zeaxanthin-independent. Photosynth Res 35:67–78. https://doi.org/10.1007/BF02185412

Grossman AR, Schaefer MR, Chiang GG, Collier JL (1994) The responses of cyanobacteria to environmental conditions: light and nutrients. In: Bryant DA (ed) Advances in photosynthesis. The molecular biology of cyanobacteria. Kluwer Academic, Dordrecht, pp 641–675

Guadagno CR, Ewers BE, Weinig C (2018) Circadian rhythms and redox state in plants: till stress do us part. Front Plant Sci 9:247. https://doi.org/10.3389/fpls.2018.00247

Haehnel W (1984) Photosynthetic electron transport in higher plants. Ann Rev Plant Physiol 35:659–693

Hendrickson L, Furbank RT, Chow WS (2004) A simple alternative approach to assessing the fate of absorbed light energy using chlorophyll fluorescence. Photosynth Res 82:73–81

Hollis L, Hüner NPA (2017) Exposure of high-light-grown cultures of Chlorella vulgaris to darkness inhibits the relaxation of excitation pressure: uncoupling of the redox state of the photosynthetic electron transport chain and phenotypic plasticity. Botany 95:1125–1140. https://doi.org/10.1139/cjb-2017-0066

Horton P, Ruban A (2005) Molecular design of the photosystem II light-harvesting antenna: photosynthesis and photoprotection. J Exp Bot 56:365–373

Horton P, Ruban A, Walters RG (1996) Regulation of light harvesting in green plants. Ann Rev Plant Physiol 47:655–684

Humby PL, Cunningham ML, Saunders HL, Price JA, Durnford DG (2009) Compartmental cross-talk in the regulation of light harvesting complex transcription under short-term light and temperature stress in Chlamydomonas reinhardtii. Botany 87:375–386. https://doi.org/10.1139/B09-005

Hüner NPA, Öquist G, Sarhan F (1998) Energy balance and acclimation to light and cold. Trends Plant Sci 3:224–230. https://doi.org/10.1016/S1360-1385(98)01248-50

Hüner NPA, Öquist G, Melis A (2003) Photostasis in plants, green algae and cyanobacteria: the role of light harvesting antenna complexes. In: Green BR, Parson WW (eds) Advances in

photosynthesis and respiration, light harvesting antennas in photosynthesis, vol 13. Kluwer Academic Publishers, Dordrecht, pp 401–421

Hüner NPA, Ivanov AG, Sane PV, Pocock T, Krol M, Balseris A, Rosso D, Savitch LV, Hurry VM, Öquist G (2005) Photoprotection of photosystem II: reaction centre quenching versus antenna quenching. In: Demming-Adams B, Adams WW III, Mattoo AK (eds) Advances in photosynthesis and respiration: photoprotection, photoinhibition, gene regulation and environment, vol 21. Springer, Dordrecht, pp 155–173

Hüner NPA, Bode R, Dahal K, Hollis L, Rosso D, Król M, Ivanov AG (2012) Chloroplast redox imbalance governs phenotypic plasticity: the "grand design of photosynthesis" revisited. Front Plant Sci 3:255. https://doi.org/10.3389/fpls.2012.00255

Hüner NPA, Bode R, Daha K, Busch FA, Possmayer M, Szyszka B, Rosso D, Ensminger I, Krol M, Ivanov AG, Maxwell DP (2013) Shedding some light on cold acclimation, cold adaptation, and phenotypic plasticity. Botany 91:127–136. https://doi.org/10.1139/cjb-2012-0174

Hüner NPA, Dahal K, Bode R, Kurepin LV, Ivanov AG (2016) Photosynthetic acclimation, vernalization, crop productivity and 'the grand design of photosynthesis'. J Plant Physiol 203:29–43. https://doi.org/10.1016/j.jplph.2016.04.006

Im CS, Grossman AR (2001) Identification and regulation of highlight-induced genes in *Chlamydomonas reinhardtii*. Plant J 30:301–313

Ivanov AG, Sane P, Hurry V, Król M, Sveshnikov D, Huner NPA, Öquist G (2003) Low temperature modulation of the redox properties of the acceptor side of photosystem II: photoprotection through reaction centre quenching of excess energy. Physiol Plant 119:376–383

Jahns P, Holzwarth AR (2012) The role of the xanthophyll cycle and of lutein in photoprotection of photosystem II. Biochim Biophys Acta 1817:182–193. https://doi.org/10.1016/j.bbabio.2011.04.012

Jeffrey SW, Humphrey GF (1975) New spectrophotometric equations for determining chlorophyll a, b, c1, c2 in higher plants, algae and natural phytoplankton. Biochem Physiol. Pflanz 167:191–194

Karpinski S, Reynolds H, Karpinska B, Wingsle G, Creissen G, Mullineaux P (1999) Systemic signaling and acclimation in response to excess excitation energy in Arabidopsis. Science 284:654–657

Ke B (2001) Photosynthesis. Photobiochemistry and photobiophysics. In: Ke B (ed) Advances in photosynthesis, vol 10. Kluwer Academic Publishers, Dordrecht

Kianianmomeni A, Hallmann A (2014) Algal photoreceptors: in vivo functions and potential applications. Planta 239:1–26. https://doi.org/10.1007/s00425-013-1962-5

Koussevitzky S, Nott A, Mockler TC, Hong F, Sachetto-Martins G, Surpin M, Lim J, Mittler R, Chory J (2007) Signals from chloroplasts converge to regulate nuclear gene expression. Science 316:715–719. https://doi.org/10.1126/science.1140516

Król M, Maxwell DP, Hüner NPA (1997) Exposure of *Dunaliella salina* to low temperature mimics the high light-induced accumulation of carotenoids and the carotenoid binding protein (Cbr). Plant Cell Physiol 38:213–216

Kurepin LV, Dahal KP, Savitch LV, Singh J, Bode R, Ivanov AG, Hurry V, Hüner NPA (2013) Role of CBFs as integrators of chloroplast redox, phytochrome and plant hormone signaling during cold acclimation. Int J Mol Sci 14:12729–12763. https://doi.org/10.3390/ijms140612729

Laemmli U (1970) Cleavage of structural proteins during the assmebly of the head of bacteriophage T4. Nature 227:680–685

Laroche J, Mortain-Bertrand A, Falkowski PG (1991) Light intensity-induced changes in cab mRNA and light harvesting complex II apoprotein levels in the unicellular chlorophyte *Dunaliella tertiolecta*. Plant Physiol 97:147–153

Lepisto A, Kangasjarvi S, Luomala E-M, Brader G, Sipari N, Keränen M, Keinänen M, Rintamäki E (2009) Chloroplast NADPH-thioredoxin reductase interacts with photoperiodic development in *Arabidopsis*. Plant Physiol 149:1261–1276. https://doi.org/10.1104/pp.108.133777

Matsuda T, Tanaka A, Melis A (2003) Chlorophyll antenna size adjustments by irradiance in *Dunaliella salina* involve coordinate regulation of chlorophyll *a* oxygenase (*CAO*) and *Lhcb* gene expression. Plant Mol Biol 51:757–771

Maxwell DP, Falk S, Trick CG, Hüner NPA (1994) Growth at low temperature mimics high-light acclimation in *Chlorella vulgaris*. Plant Physiol 105:535–543

Maxwell DP, Falk S, Hüner NPA (1995a) Photosystem II excitation pressure and development of resistance to photoinhibition. I. Light-harvesting complex II abundance and zeaxanthin content in *Chlorella vulgaris*. Plant Physiol 107:687–694. https://doi.org/10.1104/pp.107.3.687

Maxwell DP, Laudenbach DE, Hüner NPA (1995b) Redox regulation of light-harvesting complex II and *cab* mRNA abundance in *Dunaliella salina*. Plant Physiol 109:787–795

McClung CR (2006) Plant circadian rhythms. Plant Cell 18:792–803. https://doi.org/10.1105/tpc.106.040980

Melis A (1991) Dynamics of photosynthetic membrane composition and function. Biochim Biophys Acta 1058:87–106. https://doi.org/10.1016/S0005-2728(05)80225-7

Melis A (1998) Photostasis in plants. In: Williams TP, Thistle AB (eds) Photostasis and related phenomena. Plenum Press, New York, pp 207–220

Millar AJ, Straume M, Chory J, Chua NH, Kay SA (1995) The regulation of circadian period by phototransduction pathways in *Arabidopsis*. Science 267:1163–1166

Miskiewicz E, Ivanov AG, Williams JP, Khan MU, Falk S, Hüner NPA (2000) Photosynthetic acclimation of the filamentous cyanobacterium, *Plectonema boryanum* UTEX 485, to temperature and light. Plant Cell Physiol 41:767–775

Möglich A, Yang X, Ayers RA, Moffa K (2010) Structure and function of plant photoreceptors. Annu Rev Plant Biol 61:21–47. https://doi.org/10.1146/annurev-arplant-042809-112259

Murchie EH, Pinto M, Horton P (2009) Agriculture and the new challenges for photosynthesis research. New Phytol 181:532–552. https://doi.org/10.1111/j.1469-8137.2008.02705.x

Nichols SHW, Bold HC (1965) *Trichosarcina polymorpha* gen. et sp. nov. J Phycol 1:34–38

Petrillo E, Godoy-Herz MA, FuchsA Reifer D, Fuller J, Yanovsky MJ, Simpson C, Brown JWS, Barta A, Kalyna M, Kornblihtt AR (2014) A chloroplast retrograde signal regulates nuclear alternative splicing. Science 344:427–430. https://doi.org/10.1126/science.1250322

Pfannschmidt T (2003) Chloroplast redox signals: how photosynthesis controls its own genes. Trends Plant Sci 3:33–41

Pfannschmidt T, Nilsson A, Tullberg A, Link G, Allen JF (1999) Direct transcriptional control of the chloroplast genes *psbA* and *psaAB* adjusts photosynthesis to light energy distribution in plants. IUBMB Life 48:271–276. https://doi.org/10.1080/713803507

Piippo M, Allahverdiyeva Y, Paakkarinen V, Suoranta UM, Battchikova N, Aro E-M (2006) Chloroplast-mediated regulation of nuclear genes in *Arabidopsis thaliana* in the absence of light stress. Physiol Genomics 25:142–152. https://doi.org/10.1152/physiolgenomics.00256.2005

Pogson BJ, Albrecht V (2011) Genetic dissection of chloroplast biogenesis and development: an overview. Plant Physiol 155:1545–1551. https://doi.org/10.1104/pp.110.170365

Pogson BJ, Woo NS, Forster B, Small ID (2008) Plastid signalling to the nucleus and beyond. Trends Plant Sci 13:602–609. https://doi.org/10.1016/j.tplants.2008.08.008

Post AF, Dubinsky Z, Wyman K, Falkowski PG (1984) Kinetics of light-intensity adaptation in a marine planktonic diatom. Mar Biol 83:231–238

Queval G, Issakidis-Bourguet E, Hoeberichts FA, Vandorpe M, Gakière B, Vanacker H, Miginiac-Maslow M, Van Breusegem F, Noctor G (2007) Conditional oxidative stress responses in the *Arabidopsis* photorespiratory mutant *cat2* demonstrate that redox state is a key modulator of daylength-dependent gene expression, and define photoperiod as a crucial factor in the regulation of H_2O_2-induced cell death. Plant J 52:640–657. https://doi.org/10.1111/j.1365-313X.2007.03263.x

Queval G, Neukermans J, Vanderauwera S, Van Breusegem G, Noctor G (2012) Day length is a key regulator of transcriptomic responses to both CO_2 and H_2O_2 in *Arabidopsis*. Plant Cell Environ 35:374–387

Robert B, Horton P, Pascal AA, Ruban AV (2004) Insights into the molecular dynamics of plant light-harvesting proteins in vivo. Trends Plant Sci 9:385–390

Rochaix JD (2014) Regulation and dynamics of the light-harvesting system. Annu Rev Plant Biol 65:287–309. https://doi.org/10.1111/j.1365-3040.2011.02368.x

Ruban AV, Johnson MP, Duffy CDP (2012) The photoprotective molecular switch in the photosystem II antenna. Biochim Biophys Acta 1817:167–181

Ruckle ME, Larkin RM (2009) Plastid signals that affect photomorphogenesis in *Arabidopsis thaliana* are dependent on GENOMES UNCOUPLED 1 and cryptochrome 1. New Phytol. https://doi.org/10.1111/j.14698137.2008.02729.x

Ruckle ME, DeMarco SM, Larkin RM (2007) Plastid signals remodel light signaling networks and are essential for efficient chloroplast biogenesis in *Arabidopsis*. Plant Cell 19:3944–3960. https://doi.org/10.1105/tpc.107.054312

Sane PV, Ivanov AG, Öquist G, Hüner NPA (2012) Thermoluminescence. In: Eaton-Rye JJ, Tripathy BC, Sharkey TD (eds) Advances in photosynthesis and respiration. Photosynthesis: plastid biology, energy conversion and carbon assimilation, vol 34. Springer Science, Dordrecht, pp 445–474

Savitch LV, Maxwell DP, Hüner NPA (1996) Photosystem II excitation pressure and photosynthetic carbon metabolism in *Chlorella vulgaris*. Plant Physiol 111:127–136. https://doi.org/10.1104/pp.111.1.127

Shin J, Anwer MU, Davis SJ (2013) Phytochrome-interacting factors (PIFs) as bridges between environmental signals and the circadian clock: diurnal regulation of growth and development. Mol Plant 6:592–595. https://doi.org/10.1093/mp/sst060

Stewart JJ, Adams WWIII, Cohu C, Polutchko SK, Lombardi EM, Demmig-Adams B (2015) Differences in light-harvesting, acclimation to growth-light environment, and leaf structural development between Swedish and Italian ecotypes of *Arabidopsis thaliana*. Planta 242:1277–1290. https://doi.org/10.1007/s00425-015-2368-3

Sukenik A, Wyman KD, Bennett J, Falkowski PG (1987) A novel mechanism for regulating the excitation of photosystem II in a green alga. Nature 327:704–707. https://doi.org/10.1038/327704a0

Sukenik A, Bennett J, Falkowski PG (1988) Changes in the abundance of individual apoproteins of light-harvesting chlorophyll *a/b* complexes of photosystem I and II with growth irradiance in the marine chlorophyte *Dunaliella teriolecta*. Biochim Biophys Acta 932:206–215. https://doi.org/10.1016/0005-2728(88)90157-0

Tanaka A, Melis A (1997) Irradiance dependent changes in the size and composition of the chlorophyll *a-b* light harvesting complex in the green alga *Dunaliella salina*. Plant Cell Physiol 38:17–24. https://doi.org/10.1093/oxfordjournals.pcp.a029080

van Kooten O, Snel JFH (1990) The use of chlorophyll fluorescence nomenclature in the study of plant stress physiology. Photosyn Res 25:147–150

Vollsnes AV, Eriksen AB, Otterholt E, Kvaal K, Oxaal U, Futsaether CM (2009) Visible foliar injury and infrared imaging show that daylength affects short-term recovery after ozone stress in *Trifolium subterraneum*. J Exp Bot 60:3677–3686. https://doi.org/10.1093/jxb/erp213

Walters RG, Rogers JJ, Shephard F, Horton P (1999) Acclimation of *Arabidopsis thaliana* to the light environment: the role of photoreceptors. Planta 209:517–527. https://doi.org/10.1007/s004250050756

Wilson KE, Hüner NPA (2000) The role of growth rate, redox-state of the plastoquinone pool and the trans-thylakoid deltapH in photoacclimation of *Chlorella vulgaris* to growth irradiance and temperature. Planta 212:93–102

Wilson KE, Król M, Hüner NPA (2003) Temperature-induced greening of *Chlorella vulgaris*. The role of the cellular energy balance and zeaxanthin-dependent nonphotochemical quenching. Planta 217:616–627. https://doi.org/10.1007/s00425-003-1021-8

Wykoff DD, Davies JP, Melis A, Grossman AR (1998) The regulation of photosynthetic electron transport during deprivation in *Chlamydomonas reinhardtii*. Plant Physiol 117:129–139. https://doi.org/10.1104/pp.117.1.129